Microelectronic Engineering 108 (2013) 5–7

Contents lists available at SciVerse ScienceDirect

Microelectronic Engineering

journal homepage: www.elsevier.com/locate/mee

Accelerated Publication

Sub-25 nm direct write (maskless) X-ray nanolithography

Adam F.G. Leontowich [a,*], Adam P. Hitchcock [a], Ben Watts [b], Jörg Raabe [b]

[a] Brockhouse Institute for Materials Research, McMaster University, 1280 Main Street West, Hamilton, Ontario, Canada L8S 4M1
[b] Swiss Light Source, Paul Scherrer Institut, 5232 Villigen PSI, Switzerland

ARTICLE INFO

Article history:
Received 10 December 2012
Received in revised form 3 February 2013
Accepted 4 March 2013
Available online 14 March 2013

Keywords:
Maskless lithography
STXM
Fresnel zone plate
X-ray lithography
Cold development

ABSTRACT

Sub-25 nm continuous, reproducible features of arbitrary geometry were created by X-ray lithography in direct write (maskless) geometry, analogous to conventional electron beam lithography. This was achieved through the use of a laser interferometer-controlled scanning transmission X-ray microscope (STXM) equipped with a zone doubled Fresnel zone plate lens, and a cold development procedure. These features are among the smallest created with photons in direct write geometry.

1. Introduction

A focused beam of radiation can directly write on a surface like a pen moving across a sheet of paper. Computer-controlled electron and ion beams have been used extensively in this regard for fabrication on the nanometer scale, often as part of a multi-step process known as lithography. The products enabled by this technology have touched billions of people; the mass produced integrated circuits of today which are incorporated in almost everything electronic are created from sets of patterned masks, produced by directly writing them with focused electron beams [1]. Several areas of science such as X-ray microscopy and nanofluidics are highly indebted to the nano-focused electron beams used to create the enabling optics [2] and masters or devices [3], respectively. Nothing is technically preventing nano-focused X-rays from being used in like manner, but very rarely have they appeared in such roles [4]. X-ray nanofabrication has so far been limited to mask methods, particularly LIGA [5]; these approaches do not involve nano-focused X-rays. Intense nano-focused X-ray beams from synchrotrons and free-electron lasers have dramatically improved established X-ray analysis techniques and enabled many new ones [6], and could soon have a similar impact on nanofabrication. Some potential advantages of using focused X-ray beams in direct write geometry for nanofabrication include high penetration with minimal scattering for maskless deep etch lithography [5]; immunity to sample charging effects [7]; and exploitation of the energy tunability to element- or functional group-specific resonances in the sample for chemically selective patterning [8,9]. These potentials remain almost totally unexplored.

At present, there are only two published examples of sub-100 nm features directly written in free form with focused X-rays [10,11]. The "pen" in both examples was the X-rays at the focal point of a Fresnel zone plate (ZP) lens [2,12]. These optics are circular transmission gratings where the width of alternating transparent and opaque "zones" (the half periods of the grating) decreases with increasing zone radius according to the equation,

$$r_n^2 = n\lambda f$$

where r is the radius of the nth zone, λ is the wavelength of the radiation, and f is the focal length. If the numerical aperture (NA) <<1, which is often the case for X-ray ZPs including the one used for this work, then the spherical aberration correction can be dropped as shown above [2]. The design is such that the difference in path length between neighboring transparent zones to the focal point is exactly one wavelength; the diffracted radiation from each transparent zone arrives in phase and interferes constructively, forming an intense probe. Assuming that the fabrication tolerances and illumination conditions of the ZP are met or exceeded, the diffraction-limited spot diameter is directly proportional to the outer most zone width, Δr. The two previous direct write X-ray lithography results [10,11] were achieved with 25 nm Δr ZPs controlled using scanning transmission X-ray microscopes (STXM). Recent breakthroughs in X-ray ZP fabrication, specifically double patterning and zone doubling, have enabled the production of ZPs with Δr approaching 10 nm [13,14]. Here we report a record minimum

* Corresponding author. Present address: Center for Free-Electron Laser Science, Notkestraße 85, Hamburg 22607, Germany. Tel.: +49 0 40 8998 6395; fax: +49 0 40 8994 1387.
E-mail address: adam.leontowich@cfel.de (A.F.G. Leontowich).

0167-9317/$ - see front matter © 2013 Elsevier B.V. All rights reserved.
http://dx.doi.org/10.1016/j.mee.2013.03.006

feature size created with focused X-rays in direct write geometry, which was achieved using a zone doubled ZP, a laser interferometer-controlled STXM, and a cold development procedure.

2. Experimental

The ZP was supplied by the Laboratory for Micro- and Nanotechnology (LMN), Paul Scherrer Institut (PSI, Villigen, Switzerland). Very briefly, a nano-focused electron beam was used to directly write template zones in a hydrogen silsesquioxane film on a Si_3N_4 substrate. The irradiated areas become SiO_2 after a subsequent development step. A 15 nm layer of Ir was conformally deposited on the 120–150 nm thick SiO_2 template zones by atomic layer deposition, which in effect produces 15 nm wide Ir zones with half the period of the SiO_2 template [14]. The diameter D and Δr were 150 μm and 15 nm, respectively. A 2 μm thick, 60 μm diameter central stop was prepared by a second electron beam exposure. The ZP was installed in PolLux [15], the soft X-ray STXM located at the Swiss Light Source (SLS), PSI. A 40 μm order sorting aperture was installed and centered on the ZP axis to suppress undiffracted zeroth order and higher order X-rays. A schematic of the experimental arrangement is shown in Fig. 1. The sample for patterning was a 37 ± 2 nm thick film of poly(-methyl methacrylate) (PMMA, M_w = 315,000 g/mol, M_w/M_n = 1.05) on a 75 nm thick SiN (nominally Si_3N_4) substrate prepared by a spin cast and float procedure previously reported elsewhere [10]. This sample was annealed under a low vacuum (2×10^{-2} Torr) at 150 °C for 1 h. After loading the sample, the STXM chamber was pumped to 0.1 Torr and then filled with 250 Torr He. The photon energy of patterning was set at 1.0000 keV (λ = 1.24 nm) corresponding to the energy region of maximum diffraction efficiency for this ZP. The monochromator exit slit widths were set to 10 μm × 10 μm in order to exceed diffraction-limited focusing conditions given D, the photon energy and the 1.07 m exit-slit-to-ZP distance [4]. The ZP was then centered on the optical axis, assumed to be the position corresponding to the maximum detector count rate with the shutter open, by adjusting the x, y position of the STXM chamber using a girder mover system [15]. The focus of the ZP was set in the plane of the PMMA film with the assistance of sub-micrometer specimens of mica or dust in or on the film left over from the sample preparation, which are conveniently opaque to 1 keV X-rays. A defect-free area was located by cross referencing X-ray transmission images acquired with the STXM to optical micrographs of the sample. A pattern consisting of several 1 μm long lines with a pitch of 160 nm was then executed over a range of dwell times. Details of the patterning routine, instructions to create and execute patterns, and dose determination were previously reported elsewhere [16]. While the sample was being patterned the positioning of the sample fine stage (x, y) was maintained relative to the ZP to better than 10 nm (peak–valley) via a laser interferometer feedback system previously described elsewhere [17]. The feedback-control rate was greater than 200 Hz which negated the detrimental effects of low frequency vibration on patterning fidelity and minimum feature size. After patterning, the sample was removed from the chamber and developed by immersing it in a solution of 3:1 v/v isopropanol: methyl isobutyl ketone maintained at −8 °C and gently stirring for 60 s, revealing the patterned features. The developed patterned areas were imaged by atomic force microscopy (AFM) first, and later by scanning electron microscopy (SEM), to avoid artifacts introduced by SEM imaging. A 5 ± 1 nm Pt layer was sputter coated onto the sample after AFM imaging but prior to SEM imaging to eliminate resolution degradation due to charging. All feature widths were measured from the scanning electron micrographs.

3. Results

Scanning electron micrographs of the developed sample are presented in Fig. 2. Continuous 33 ± 4 nm (full width) lines of cross-linked (negative mode) PMMA were produced at a dose of 25 ± 4 MGy (Fig. 2(a)). This width includes the 5 ± 1 nm Pt coating necessary to image the features; the uncoated (as-fabricated) width is estimated to be 20–25 nm. The average height of the lines presented in Fig. 2(a) was found to be 17 ± 1 nm using AFM (Fig. 3). Doses greater than 25 MGy resulted in line widths greater than 33 nm. This increase in feature width with dose is in fact due to the point spread function of the optical system [10,18]. Lines made at a dose of 24 ± 4 MGy had an average width of 26 nm, and some were continuous over their 1 μm length (Fig. 2(b)). However, lines made with doses of 24 MGy or less were not reproducibly continuous. Lines just begin to form (i.e. onset of negative mode) at a dose of 23 ± 4 MGy (Fig. 2(c)). This is significantly lower than the 90 ± 5 MGy onset of negative mode for PMMA developed using

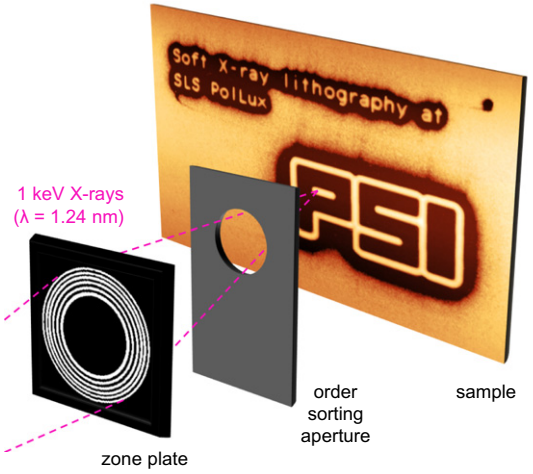

Fig. 1. Schematic depicting the experimental arrangement (color online). During patterning the zone plate and order sorting aperture are fixed while the sample is translated in x and y. The dimensions of the atomic force micrograph demonstrating arbitrary geometry patterning capability are 15 μm × 10 μm.

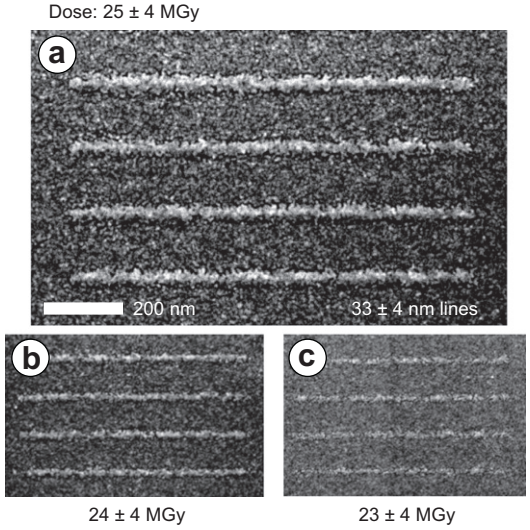

Fig. 2. Scanning electron micrographs of 1 μm long lines of cross-linked PMMA with a pitch of 160 nm, made with various doses of 1 keV X-rays. (a) Continuous 33 ± 4 nm lines, dose: 25 ± 4 MGy. (b) Discontinuous 26 nm lines, dose: 24 ± 4 MGy. (c) At a dose of 23 ± 4 MGy cross-linked lines hardly formed.

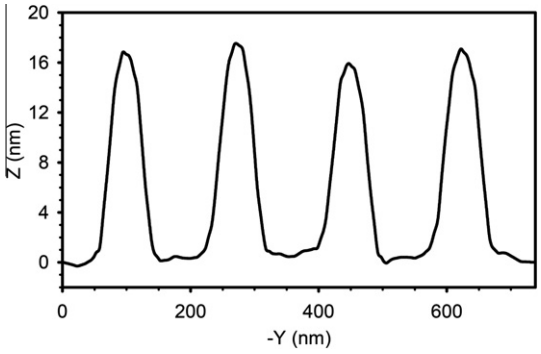

Fig. 3. Averaged AFM line trace of lines presented in Fig. 2(a), recorded before Pt coating and SEM imaging. The lines appear much wider due to tip convolution effects.

the same developer but at 20 °C [10], and is consistent with observations from electron beam lithography [19].

4. Discussion and conclusions

The lines demonstrated here are the smallest features produced with X-rays in direct write (maskless) geometry, and the smallest produced using a ZP. Furthermore, these may be the smallest *arbitrary geometry, continuous and reproducible* features produced with photons in direct write geometry. Most examples of direct write patterning with photons have involved visible wavelengths. The minimum feature width achieved is usually limited by diffraction to 100–200 nm or more, however sub-100 nm features have been achieved through several innovative approaches. Advancements in the far-field technique of multi-photon absorption polymerization have led to examples of 80 nm wide lines with 800 nm laser light [20], and 65 ± 5 nm features with 520 nm light [21]. Menon et al. demonstrated 80 nm line width capability by creating near-field apertures in a photochromic top layer using far-field exposures at wavelengths of 325 nm and 633 nm [22]. Sub-100 nm features have also been directly written with scanning near-field optical microscopes (NSOM). The smallest continuous line widths achieved using NSOMs are between 20 nm and 40 nm [23,24], but the quality and consistency appear to be inferior to what has been demonstrated here using ZP focused 1 keV X-rays. We expect to achieve even better feature quality in the near term: At this level of performance the roughness of the SiN substrate (R_q = 0.62 nm) contributes to the measured line width roughness. STXM patterning experiments are currently limited to thin X-ray transmissive substrates such as SiN as they enable accurate focusing, but patterning on smoother Si wafers ($R_q \leqslant 0.1$ nm) and other opaque samples will be possible by incorporating of a focusing procedure involving electron yield [25,26] or fluorescence detection.

Historically it has proven much more challenging to focus X-rays to nanometer dimensions compared to electrons, and the record minimum X-ray spot size may never equal that achievable with electrons. In spite of this, the minimum *feature width* achievable by both radiation types could become equivalent, possibly by the end of this decade. It has been observed that the minimum line width attainable in polymeric resists is around 5 nm, whereas the electron beams used to make such features typically have a spot size much smaller than that. This intrinsic limit is due to exposure from secondary electrons liberated within the resist by the primary beam [27]. A sub-5 nm X-ray beam should face this same limitation and therefore be capable of the same minimum feature size as present electron beam systems. X-ray optics are steadily advancing; two dimentional focusing has now reached 8 nm for hard X-rays [28], and sub-5 nm focusing is a goal at several current synchrotron beamlines [6]. Ultimately, feature sizes equal to those made by electron beams should be possible when a sub-5 nm X-ray spot (not resolution) is achieved.

Acknowledgments

The authors thank Dr. Joan Vila-Comamala for correspondence on zone plate fabrication. A.F.G.L. acknowledges financial support from an Advanced Light Source doctoral fellowship in residence. The PolLux end station was financed by the German Minister für Bildung und Forschung, contract 05 KS4We1/6.

References

[1] G.R. Brewer, Electron-Beam Technology in Microelectronic Fabrication, Academic Press, New York, 1980.
[2] M. Howells, C. Jacobsen, T. Warwick, Principles and applications of zone plate X-ray microscopes, in: P.W. Hawkes, J.C.H. Spence (Eds.), Science of Microscopy, vol. 2, Springer, New York, 2007. ch. 13.
[3] J.B. Edel, A.J. de Mello (Eds.), Nanofluidics: Nanoscience and Nanotechnology, RSC Publishing, Cambridge, 2009.
[4] A.F.G. Leontowich, Ph.D. thesis, McMaster University, Open Access Dissertations and Theses, Paper 7360, 2012.
[5] W. Ehrfeld, D. Münchmeyer, Nucl. Instrum. Methods A 303 (1991) 523–531.
[6] G.E. Ice, J.D. Budai, J.W.L. Pang, Science 334 (2011) 1234–1239.
[7] L.D. Bozano, R. Sooriyakumaran, L.K. Sundberg, M.I. Sanchez, E.M. Lofano, C.T. Rettner, T. Nagasawa, S. Watanabe, Y. Kawai, N. Palavesam, G.G. Montano, Proc. SPIE 8325 (2012) 83250X.
[8] J. Wang, H.D.H. Stöver, A.P. Hitchcock, J. Phys. Chem. C 111 (2007) 16330–16338.
[9] J. Wang, H.D.H. Stöver, A.P. Hitchcock, T. Tyliszczak, J. Synchrotron Radiat. 14 (2007) 181–190.
[10] A.F.G. Leontowich, A.P. Hitchcock, Appl. Phys. A 103 (2011) 1–11.
[11] A.G. Caster, S. Kowarik, A.M. Schwartzberg, S.R. Leone, A. Tivanski, M.K. Gilles, J. Vac. Sci. Technol. B 28 (2010) 1304–1313.
[12] A.G. Michette, Optical Systems for Soft X Rays, Plenum, New York, 1986.
[13] W. Chao, P. Fischer, T. Tyliszczak, S. Rekawa, E. Anderson, P. Naulleau, Opt. Express 20 (2012) 9777–9783.
[14] J. Vila-Comamala, K. Jefimovs, J. Raabe, T. Pilvi, R.H. Fink, M. Senoner, A. Maaβdorf, M. Ritala, C. David, Ultramicroscopy 109 (2009) 1360–1364.
[15] J. Raabe, G. Tzvetkov, U. Flechsig, M. Böge, A. Jaggi, B. Sarafimov, M.G.C. Vernooij, T. Huthwelker, H. Ade, D. Kilcoyne, T. Tyliszczak, R.H. Fink, C. Quitmann, Rev. Sci. Instrum. 79 (2008) 113704.
[16] A.F.G. Leontowich, A.P. Hitchcock, T. Tyliszczak, M. Weigand, J. Wang, C. Karunakaran, J. Synchrotron Radiat. 19 (2012) 976–987.
[17] A.L.D. Kilcoyne, T. Tyliszczak, W.F. Steele, S. Fakra, P. Hitchcock, K. Franck, E. Anderson, B. Harteneck, E.G. Rightor, G.E. Mitchell, A.P. Hitchcock, L. Yang, T. Warwick, H. Ade, J. Synchrotron Radiat. 10 (2003) 125–136.
[18] A.F.G. Leontowich, T. Tyliszczak, A.P. Hitchcock, Proc. SPIE 8077 (2011) 80770N.
[19] B. Cord, J. Lutkenhaus, K.K. Berggren, J. Vac. Sci. Technol. B 25 (2007) 2013–2016.
[20] L. Li, R.R. Gattass, E. Gershgoren, H. Hwang, J.T. Fourkas, Science 324 (2009) 910–913.
[21] W. Haske, V.W. Chen, J.M. Hales, W. Dong, S. Barlow, S.R. Marder, J.W. Perry, Opt. Express 15 (2007) 3426–3436.
[22] T.L. Andrew, H. Tsai, R. Menon, Science 324 (2009) 917–921.
[23] S. Sun, G.J. Leggett, Nano Lett. 4 (2004) 1381–1384.
[24] N. Murphy-DuBay, L. Wang, E.C. Kinzel, S.M.V. Uppuluri, X. Xu, Opt. Express 16 (2008) 2584–2589.
[25] D. Nolle, M. Weigand, G. Schütz, E. Goering, Microsc. Microanal. 17 (2011) 834–842.
[26] B. Watts, H. Ade, Mater. Today 15 (2012) 148–157.
[27] A.N. Broers, A.C.F. Hoole, J.M. Ryan, Microelectron. Eng. 32 (1996) 131–142.
[28] K. Yamauchi, H. Mimura, T. Kimura, H. Yumoto, S. Handa, S. Matsuyama, K. Arima, Y. Sano, K. Yamamura, K. Inagaki, H. Nakamori, J. Kim, K. Tamasaku, Y. Nishino, M. Yabashi, T. Ishikawa, J. Phys.: Condens. Matter 23 (2011) 394206.